NACA RM A52C10a

NACA

RESEARCH MEMORANDUM

LIFT, DRAG, AND PITCHING MOMENT OF LOW-ASPECT-RATIO WINGS AT SUBSONIC AND SUPERSONIC SPEEDS - PLANE TRIANGULAR WING OF ASPECT RATIO 3 WITH AIR-TO-AIR MISSILE MODELS MOUNTED EXTERNALLY

By Donald Conrard

Ames Aeronautical Laboratory
Moffett Field, Calif.

NATIONAL ADVISORY COMMITTEE FOR AERONAUTICS

WASHINGTON

June 26, 1952
Declassified March 19, 1957

NATIONAL ADVISORY COMMITTEE FOR AERONAUTICS

RESEARCH MEMORANDUM

LIFT, DRAG, AND PITCHING MOMENT OF LOW-ASPECT-RATIO WINGS AT SUBSONIC AND SUPERSONIC SPEEDS - PLANE TRIANGULAR WING OF ASPECT RATIO 3 WITH AIR-TO-AIR MISSILE MODELS MOUNTED EXTERNALLY

By Donald Conrard

SUMMARY

This report presents results of an investigation of effects of externally mounted missile models on the aerodynamic characteristics of a triangular wing of aspect ratio 3 at both subsonic and supersonic Mach numbers. The lift, drag, and pitching moment of the wing-fuselage model fitted with the missile models are presented for Mach numbers of 0.6, 0.9, 1.2, 1.4, and 1.7 at a Reynolds number of 4.8 million. Similar data are presented for the basic wing.

INTRODUCTION

A research program is in progress at the Ames Aeronautical Laboratory to ascertain experimentally at subsonic and supersonic Mach numbers the characteristics of wings of interest in the design of high-speed fighter airplanes. The present report is concerned with the influence of externally mounted missiles on the characteristics of a wing-body combination incorporating a plane triangular wing of aspect ratio 3. The model is the same as that used in reference 1. The present investigation was limited to tests of the basic wing and the basic wing fitted with six models of an air-to-air missile of the beam-rider type and, alternately, eight models of an air-to-air missile of a passive-seeker type.

As in reference 1, the data herein are presented without analysis to expedite publication.

NOTATION

b	wing span
$\bar{c}$	mean aerodynamic chord $\left(\frac{\int_0^{b/2} c^2 dy}{\int_0^{b/2} c\, dy}\right)$
c	local wing chord
l	length of body including portion removed to accommodate sting
$\frac{L}{D}$	lift-drag ratio
$\left(\frac{L}{D}\right)_{max}$	maximum lift-drag ratio
M	Mach number
q	free-stream dynamic pressure
R	Reynolds number based on the mean aerodynamic chord
r	radius of body
r_o	maximum body radius
S	total wing area, including area formed by extending leading and trailing edges to plane of symmetry
x	longitudinal distance from nose of body
y	distance perpendicular to plane of symmetry
α	angle of attack of body axis, degrees
C_D	drag coefficient $\left(\frac{\text{drag}}{qS}\right)$
ΔC_D	incremental drag coefficient of externally stored missile models based on wing area S
C_L	lift coefficient $\left(\frac{\text{lift}}{qS}\right)$

C_m pitching-moment coefficient referred to quarter point of mean aerodynamic chord $\left(\frac{\text{pitching moment}}{qS\bar{c}}\right)$

$\frac{dC_L}{d\alpha}$ slope of the lift curve measured at zero lift, per degree

$\frac{dC_m}{dC_L}$ slope of the pitching-moment curve measured at zero lift

APPARATUS

Wind Tunnel and Equipment

The experimental investigation was conducted in the Ames 6- by 6-foot supersonic wind tunnel. In this wind tunnel, the Mach number can be varied continuously and the stagnation pressure can be regulated to maintain a given test Reynolds number. The air is dried to prevent formation of condensation shocks. Further information on this wind tunnel is presented in reference 2.

The model was sting mounted in the tunnel, the diameter of the sting being about 93 percent of the diameter of the body base. The pitch plane of the model support was horizontal. A 4-inch-diameter, four-component, strain-gage balance (described in reference 3), enclosed within the body of the model, was used to measure the aerodynamic forces and moments.

Model

A photograph of the model is given in figure 1. Figures 2, 3, 4, and 5 give important dimensions of the basic wing, the missile models, and the arrangement of the missile models on the triangular wing.

Wing

Aspect ratio	3
Taper ratio	0
Airfoil section (streamwise)	NACA 0003-63
Total area, S, square feet	2.425
Mean aerodynamic chord, $\bar{c}$, feet	1.199
Dihedral, degrees	0
Camber	None
Twist, degrees	0
Incidence, degrees	0
Distance, wing-chord plane to body axis, feet	0

Body

Fineness ratio (based upon length l; fig. 2)	12.5
Cross-section shape	Circular
Maximum cross-sectional area, square feet	0.1235
Ratio of maximum cross-sectional area to wing area	0.0509

The model wing was constructed of solid steel and the model fuselage consisted of a steel spar covered with aluminum which formed the body contours; the surface of the wing and body were polished smooth.

The missile models were constructed entirely of steel.

TESTS AND PROCEDURE

Range of Test Variables

The characteristics of the model (as a function of angle of attack) were investigated for Mach numbers of 0.6, 0.9, 1.2, 1.4, and 1.7. The data were obtained at a constant Reynolds number of 4.8 million.

Reduction of Data

The test data have been reduced to standard NACA coefficient form. Factors which could affect the accuracy of these results, together with the corrections applied, are discussed in the following paragraphs.

Tunnel-wall interference.- Corrections to the subsonic results for the induced effects of the tunnel walls resulting from lift on the model were made according to the methods of reference 4. The numerical values of these corrections (which were added to the uncorrected data) were:

$$\Delta\alpha = 0.554\ C_L$$

$$\Delta C_D = 0.0097\ C_L^2$$

No corrections were made to the pitching-moment coefficients.

The effects of constriction of the flow at subsonic speeds by the tunnel walls were taken into account by the method of reference 5. This correction was calculated for conditions at zero angle of attack and was applied throughout the angle-of-attack range. At a Mach number of 0.90, this correction amounted to a 2-percent increase in the Mach number and in the dynamic pressure over that determined from a calibration of the wind tunnel without a model in place.

For the tests at supersonic speeds, the reflection from the tunnel walls of the Mach wave originating at the nose of the body did not cross the model. No corrections were required, therefore, for tunnel-wall effects.

Stream variations.- Tests at subsonic speeds in the 6- by 6-foot supersonic wind tunnel of the present symmetrical model in both the normal and inverted positions have indicated a stream inclination of -0.05° and a stream curvature capable of producing a pitching-moment coefficient of -0.004 at zero lift. No corrections were made to the data of the present report for the effect of these stream irregularities. No measurements have been made of the stream curvature in the yaw plane. At subsonic speeds, the longitudinal variation of static pressure in the region of the model is not known accurately at present, but a preliminary survey has indicated that it is less than 2 percent of the dynamic pressure. No correction for this effect was made.

A survey of the air stream in the 6- by 6-foot wind tunnel at supersonic speeds (reference 2) has shown a stream curvature only in the yaw plane of the model. The effects of this curvature on the measured characteristics of the present model are not known but are believed to be small as judged by the results of reference 6. The survey of reference 2 also indicated that there is a static-pressure variation in the test section of sufficient magnitude to affect the drag results. A correction was added to the measured drag

coefficient, therefore, to account for the longitudinal buoyancy caused by this static-pressure variation. This correction varied from 0.0002 at a Mach number of 1.2 to 0.0006 at a Mach number of 1.7.

Support interference.- At subsonic speeds, the effects of support interference on the aerodynamic characteristics of the model are not known. For the present tailless model, it is believed that such effects consisted primarily of a change in the pressure at the base of the model. In an effort to correct at least partially for this support interference, the base pressure was measured and the drag data were adjusted to correspond to a base pressure equal to the static pressure of the free stream.

At supersonic speeds, the effects of support interference of a body-sting configuration similar to that of the present model are shown by reference 7 to be confined to a change in base pressure. The previously mentioned adjustment of the drag for base pressure, therefore, was applied at supersonic speeds.

RESULTS

The results are presented in this report without analysis in order to expedite publication. The variation of lift coefficient with angle of attack and the variation of pitching-moment coefficient, drag coefficient, and lift-drag ratio with lift coefficient at Mach numbers from 0.6 to 1.7 and at a Reynolds number of 4.8 million are given in figures 6, 7, and 8. The data in figure 6 are those obtained with the large air-to-air missile models (beam-rider type) mounted in an unbanked position below the model wing in both the fore and aft positions on the model wing. Figure 7 presents similar results for the large missile model banked 45° when positioned below the wing. Figure 8 shows similar data for the small air-to-air missile for the two chordwise positions on the wing.

The incremental drag coefficients for the two missile models in the two chordwise positions for two lift coefficients are given in figures 9 and 10, and the maximum lift-drag ratio as a function of Mach number is given for all the arrangements in figure 11.

In all cases, the aerodynamic characteristics of the basic wing are presented for comparison where appropriate.

Ames Aeronautical Laboratory
National Advisory Committee for Aeronautics
Moffett Field, Calif.

REFERENCES

1. Heitmeyer, John C.: Lift, Drag, and Pitching Moment of Low-Aspect-Ratio Wings at Subsonic and Supersonic Speeds - Plane Triangular Wing of Aspect Ratio 3 With NACA 0003-63 Section. NACA RM A51H02, 1951.

2. Frick, Charles W., and Olson, Robert N.: Flow Studies in the Asymmetric Adjustable Nozzle of the Ames 6- by 6-Foot Supersonic Wind Tunnel. NACA RM A9E24, 1949.

3. Olson, Robert N., and Mead, Merrill H.: Aerodynamic Study of a Wing-Fuselage Combination Employing a Wing Swept Back 63°.- Effectiveness of an Elevon as a Longitudinal Control and the Effects of Camber and Twist on the Maximum Lift-Drag Ratio at Supersonic Speeds. NACA RM A50A13a, 1950.

4. Glauert, H.: Wind Tunnel Interference on Wings, Bodies and Airscrews. R. & M. No. 1566, British A.R.C., 1933.

5. Herriot, John G.: Blockage Corrections for Three-Dimensional-Flow Closed-Throat Wind Tunnels, with Consideration of the Effect of Compressibility. NACA Rep. 995, 1950. (Formerly NACA RM A7B28)

6. Lessing, Henry C.: Aerodynamic Study of a Wing-Fuselage Combination Employing a Wing Swept Back 63° - Effect of Sideslip on Aerodynamic Characteristics at a Mach Number of 1.4 With the Wing Twisted and Cambered. NACA RM A50F09, 1950.

7. Perkins, Edward W.: Experimental Investigation of the Effects of Support Interference on the Drag of Bodies of Revolution at a Mach Number of 1.5. NACA TN 2292, 1951.

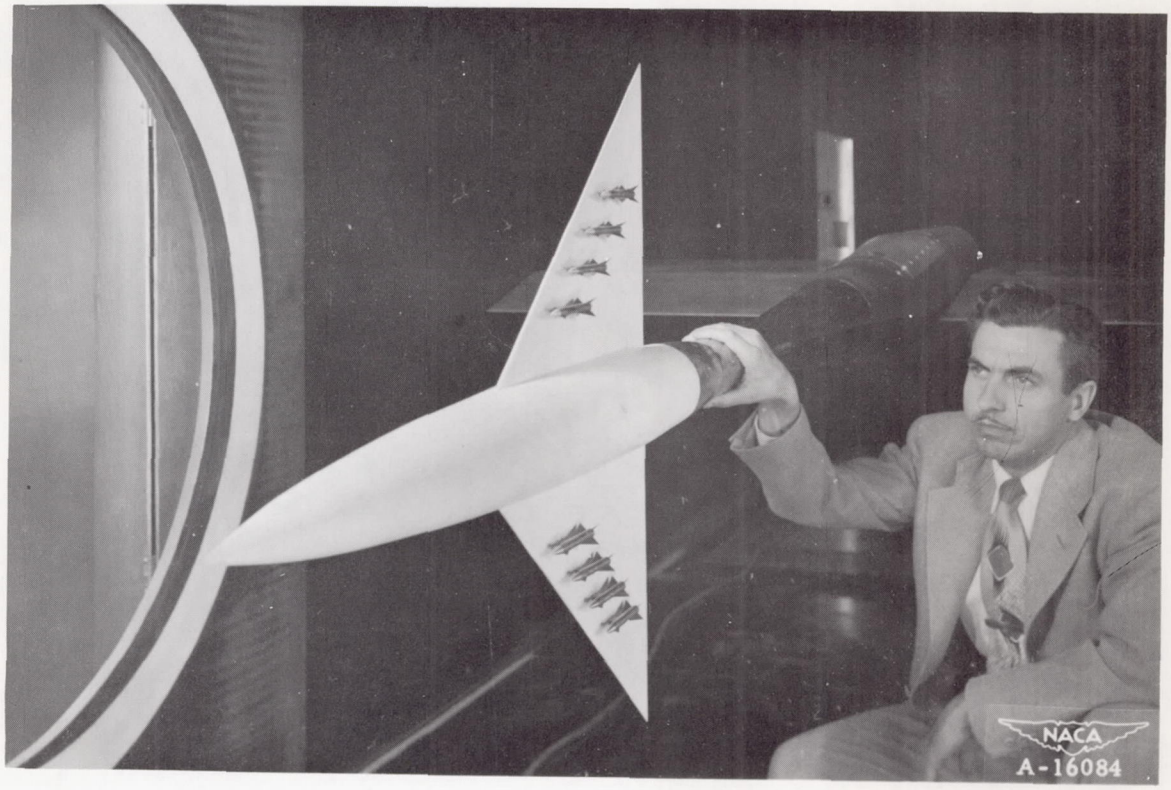


Figure 1.- Photograph of the model mounted in the test section of the wind tunnel with small missiles in the forward position.

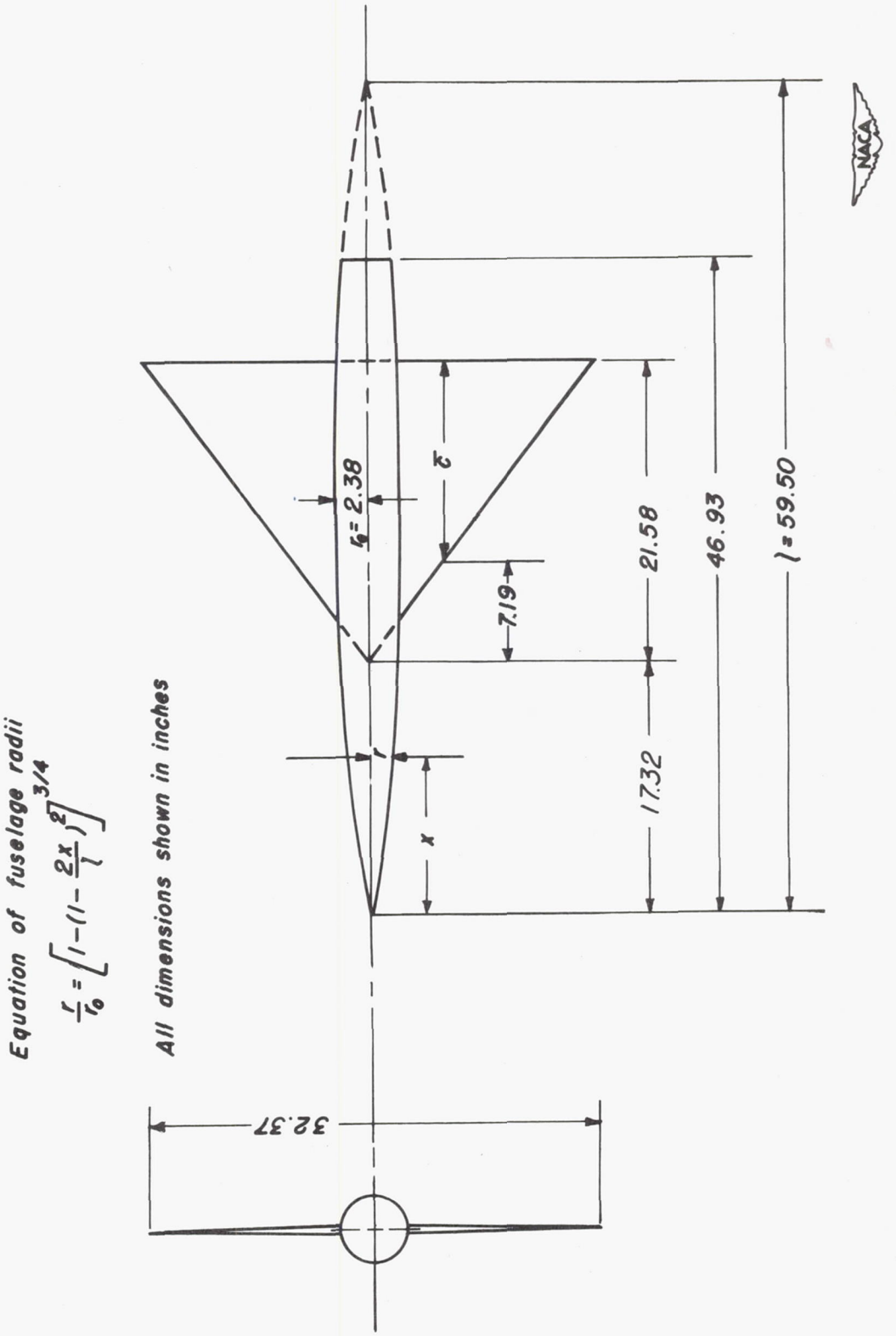
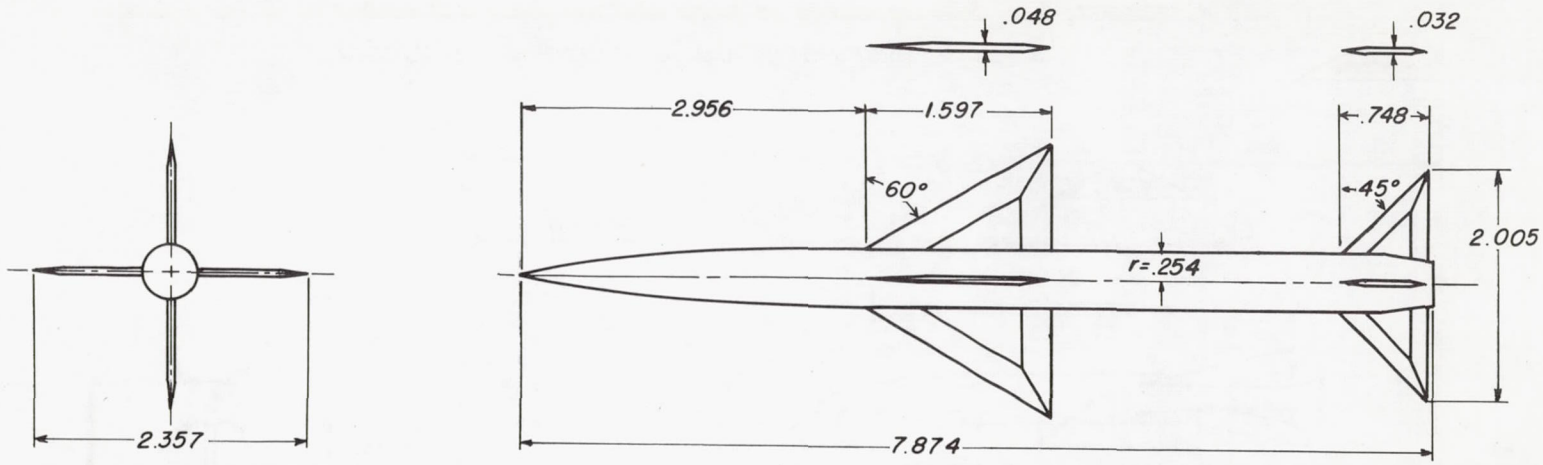
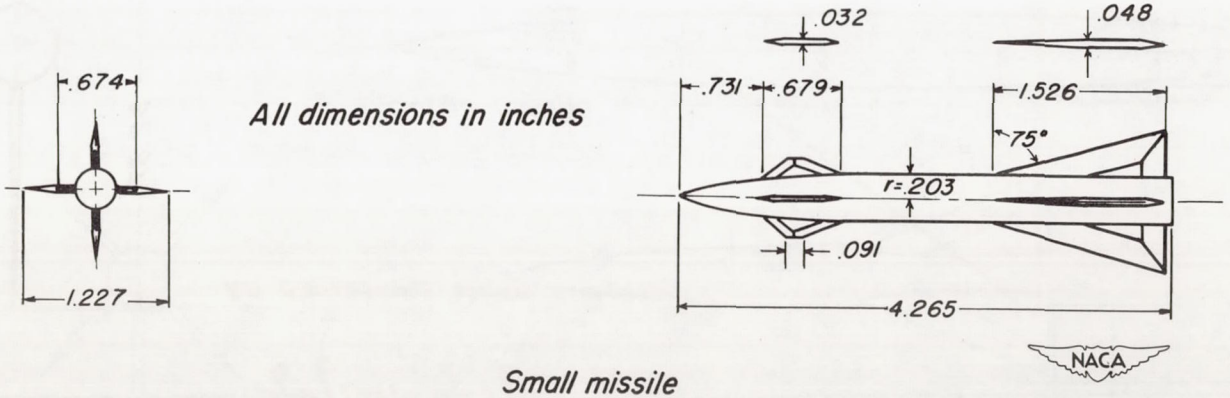


Figure 2. - Front and plan views of the model wing and fuselage.



Large missile



All dimensions in inches

Small missile

Figure 3. – Air-to-air missile models utilized in the investigation.

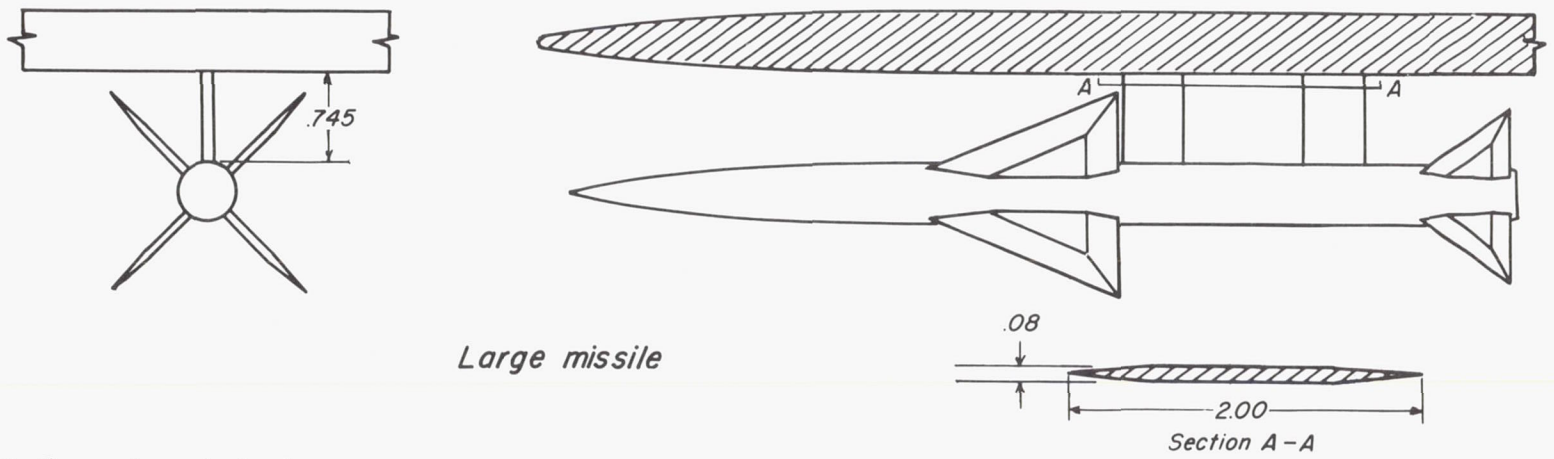


Figure 4 . – Method of mounting missile models .

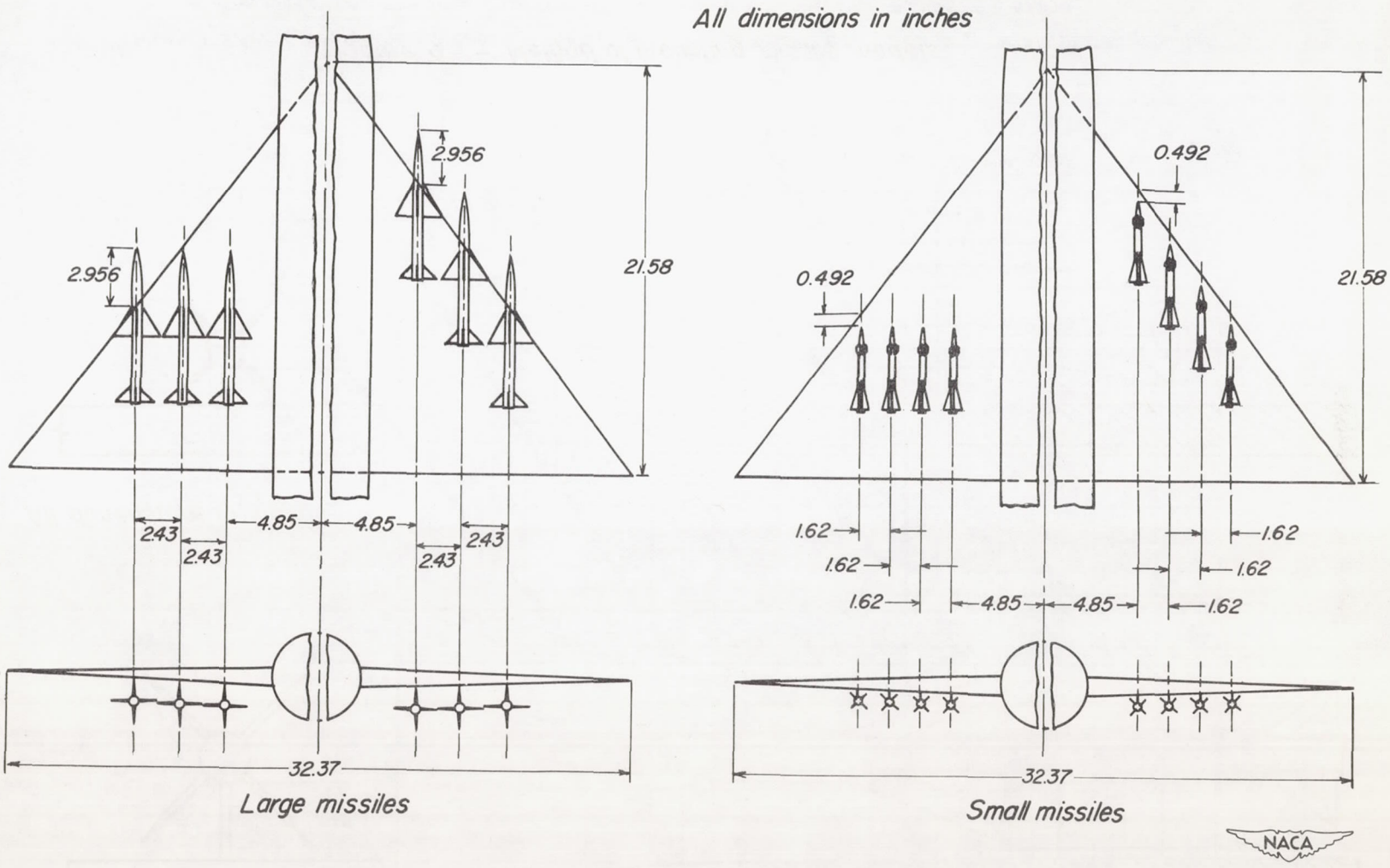
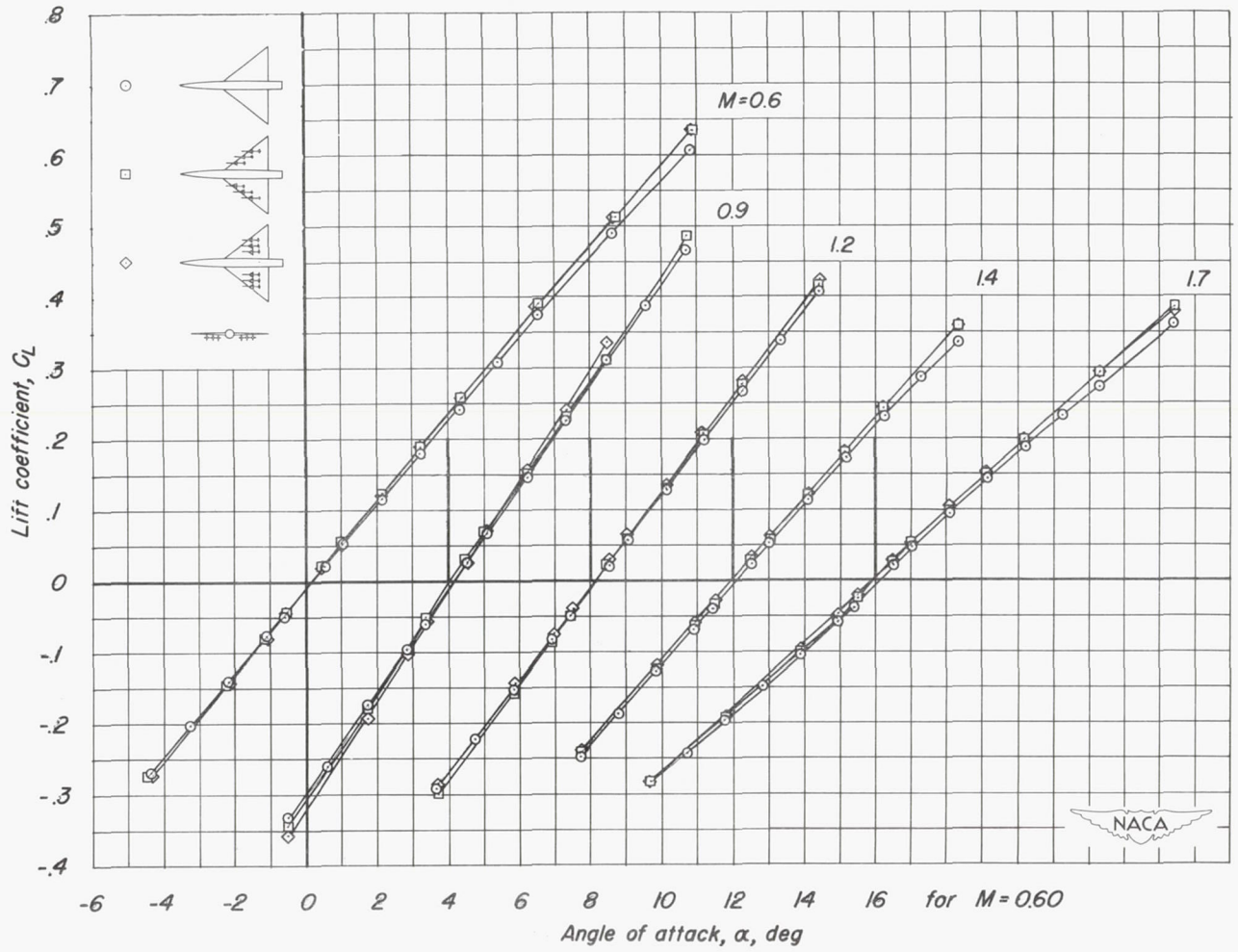
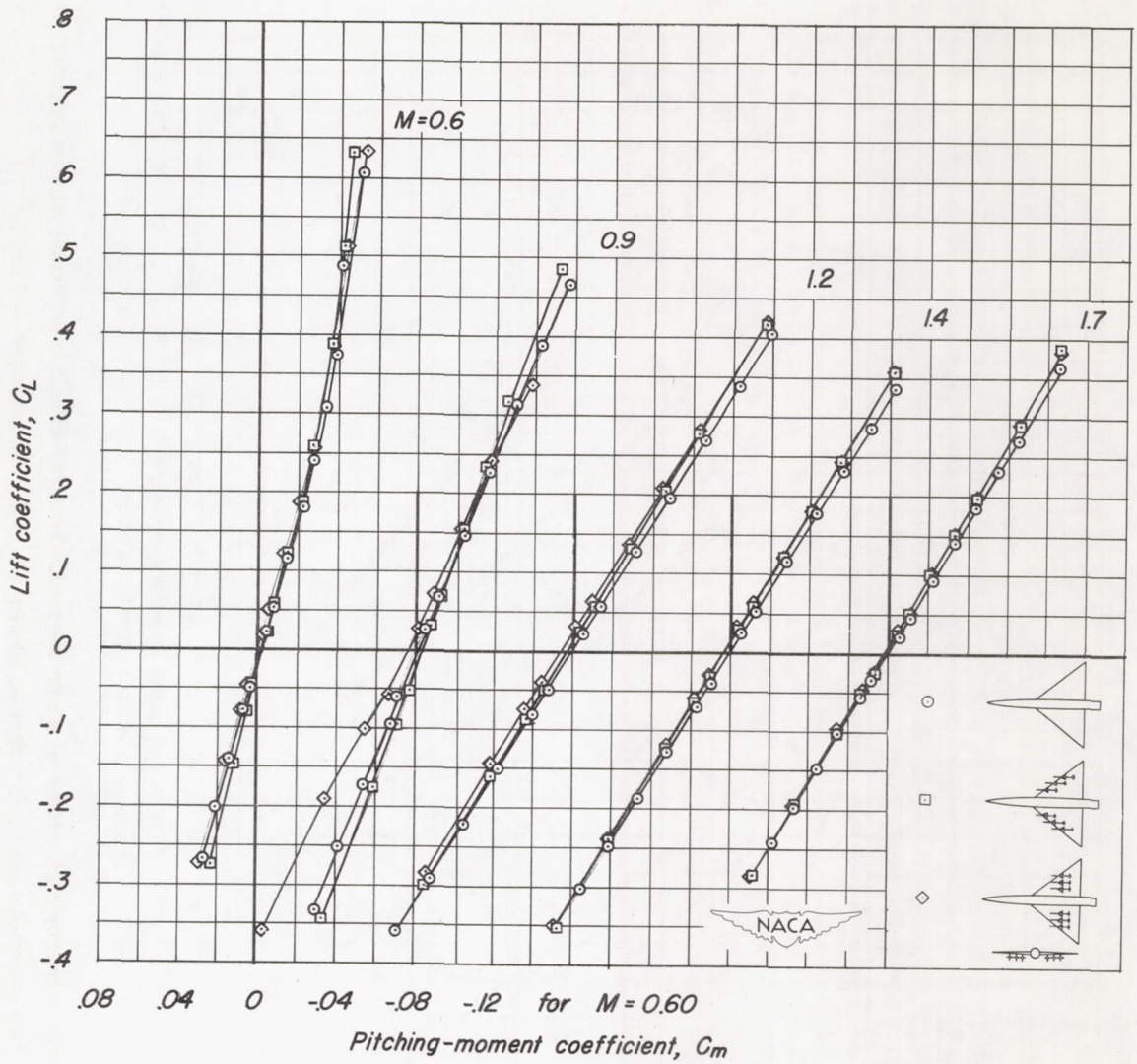


Figure 5. — Arrangement of missile models beneath model wing in both forward and rearward locations.



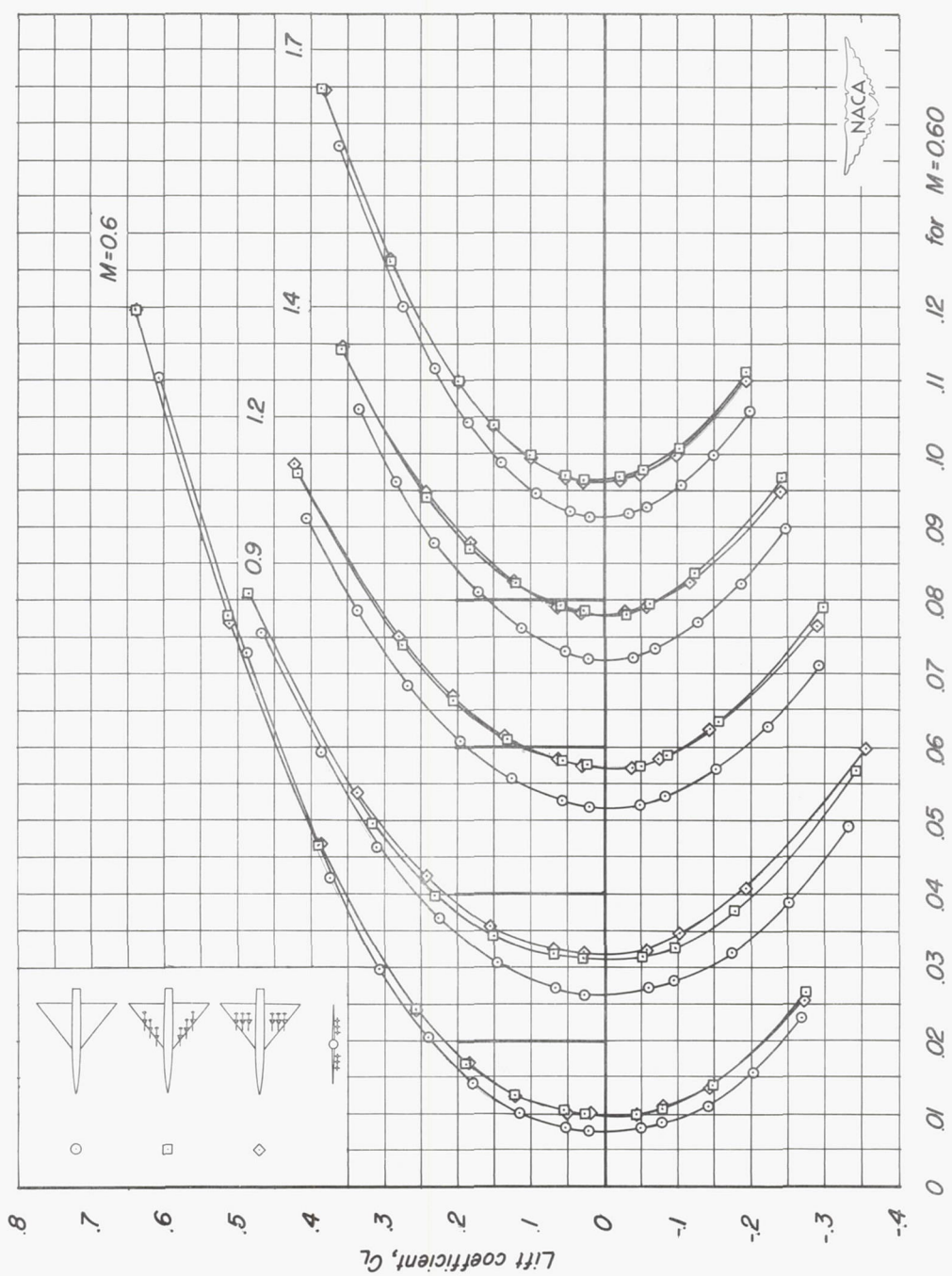
(a) C_L vs α

Figure 6.- Aerodynamic characteristics of the triangular wing model with and without large missile models mounted externally in two chordwise positions. Missiles banked 0°. Reynolds number, 4.8 million.



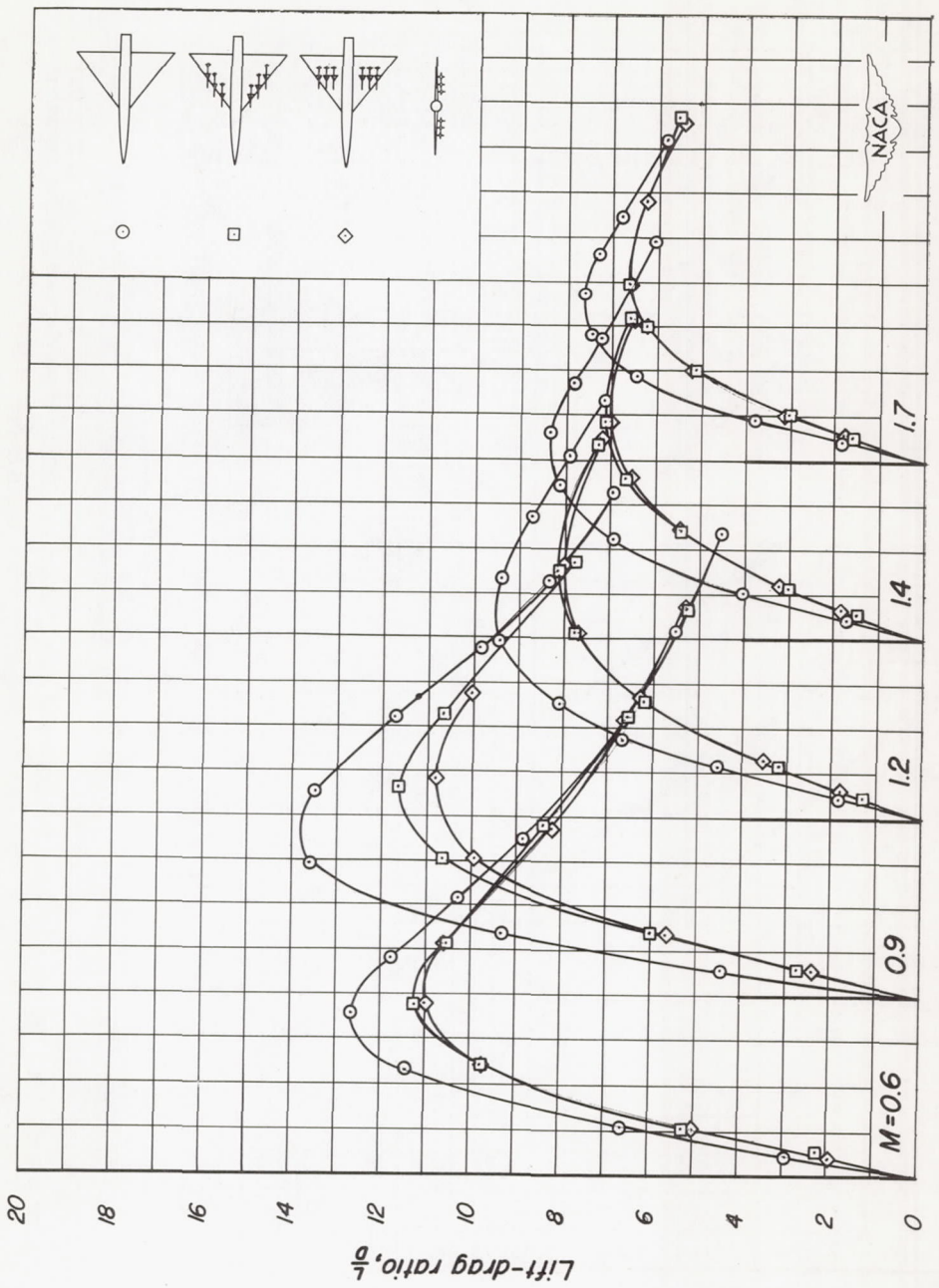
(b) C_L vs C_m

Figure 6. – Continued.



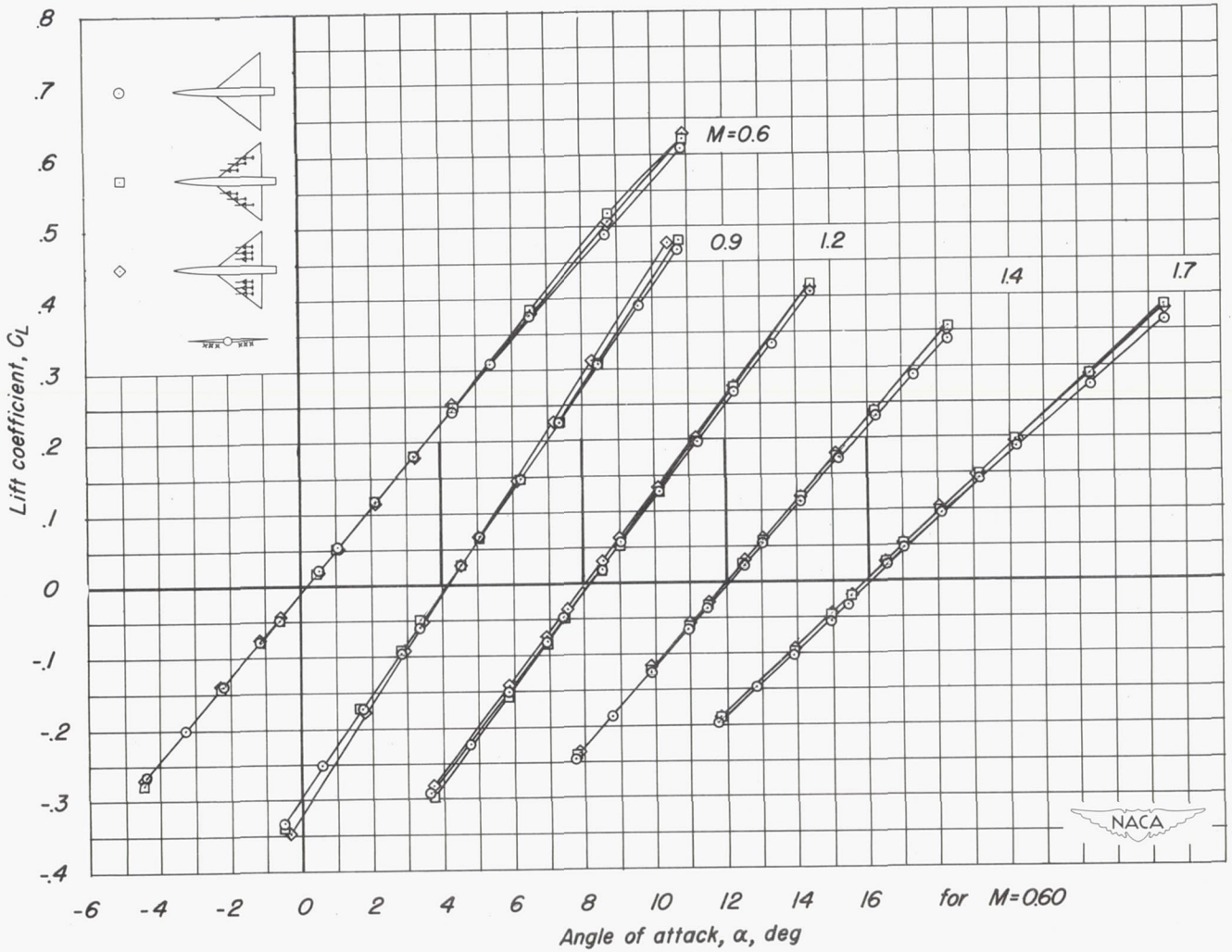
(c) C_L vs C_D

Figure 6.–Continued.



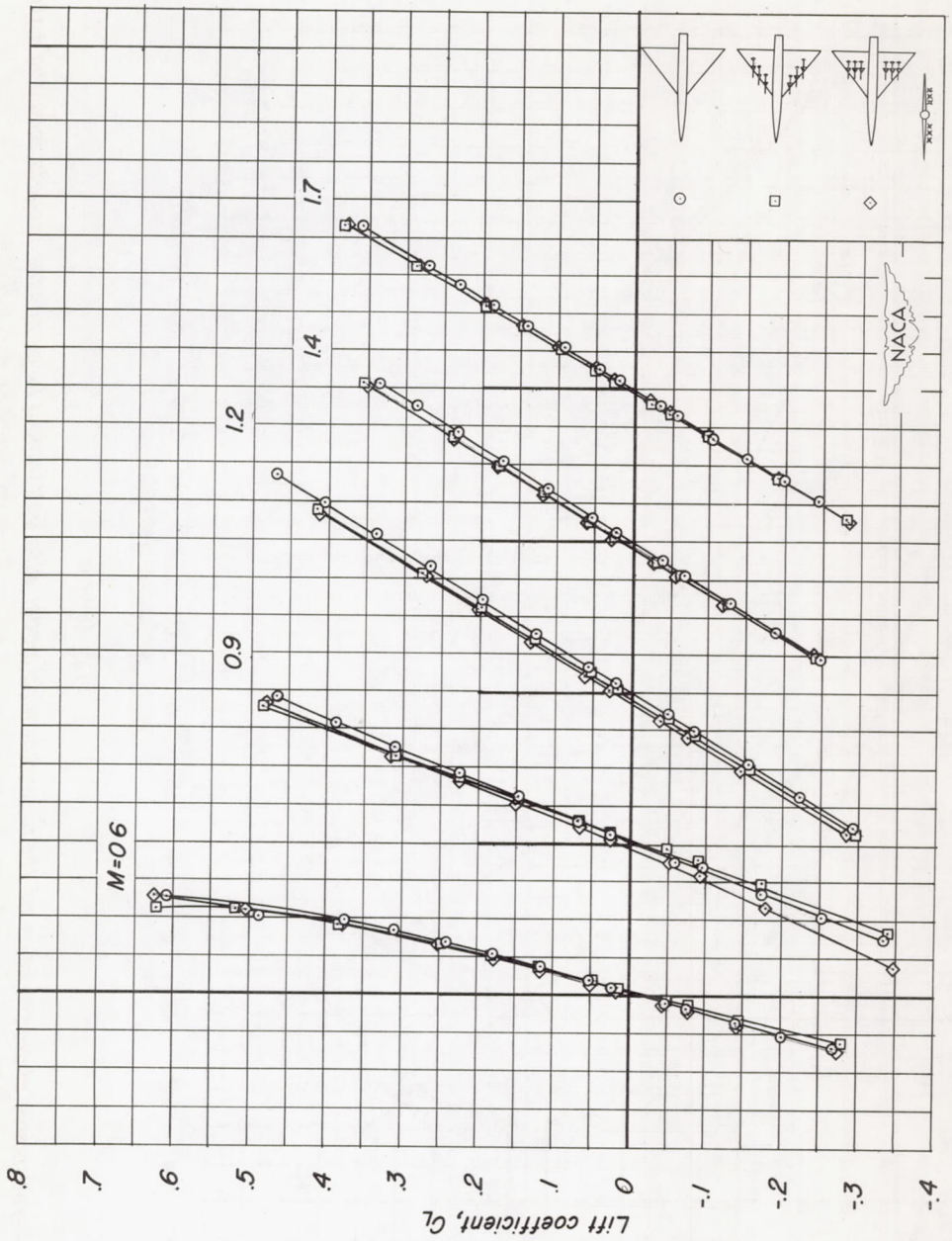
(d) C_L vs $\frac{L}{D}$

Figure 6.– Concluded.



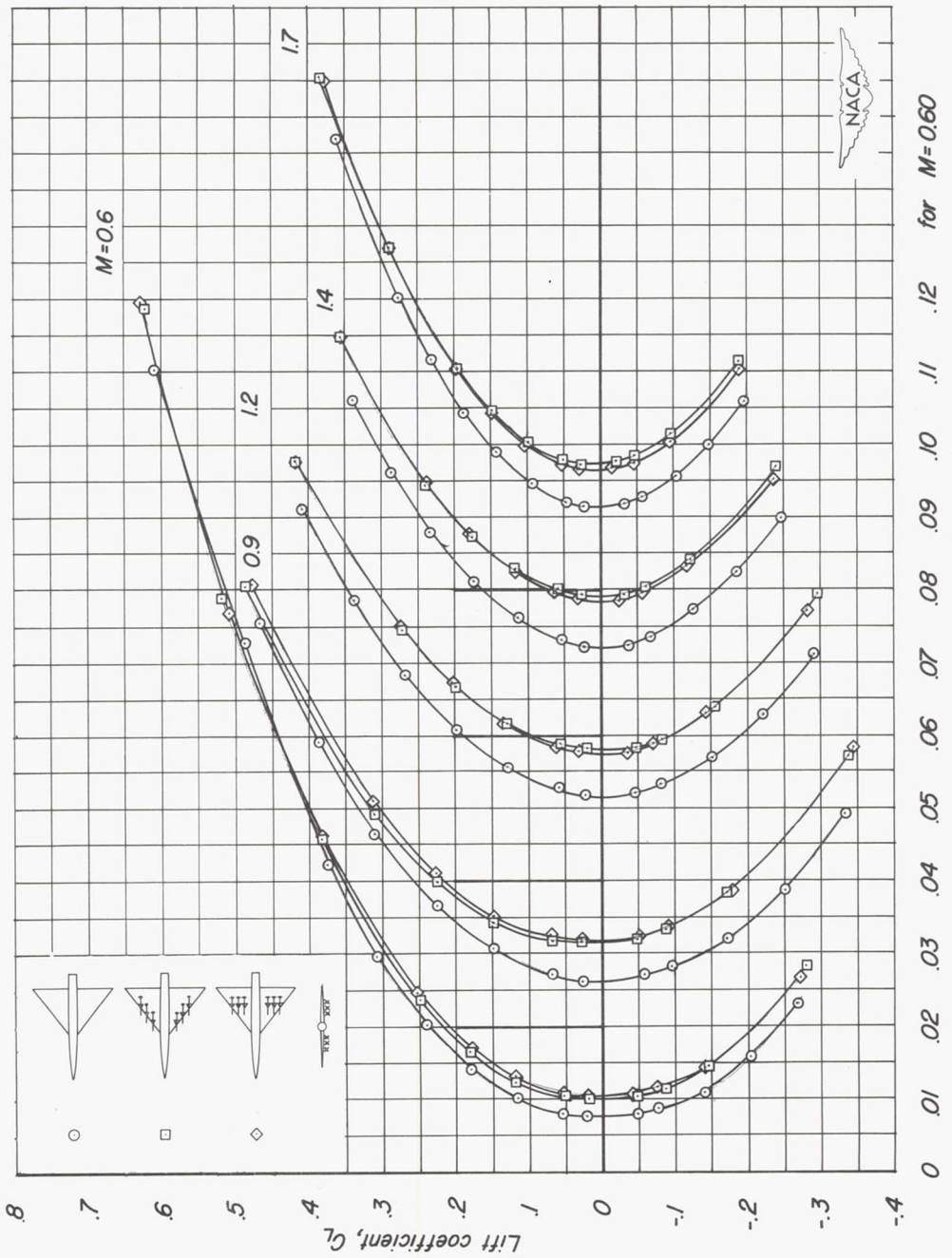
(a) C_L vs α

Figure 7. – Aerodynamic characteristics of the triangular wing model with and without large missile models mounted externally in two chordwise positions. Missiles banked 45°. Reynolds number, 4.8 million.



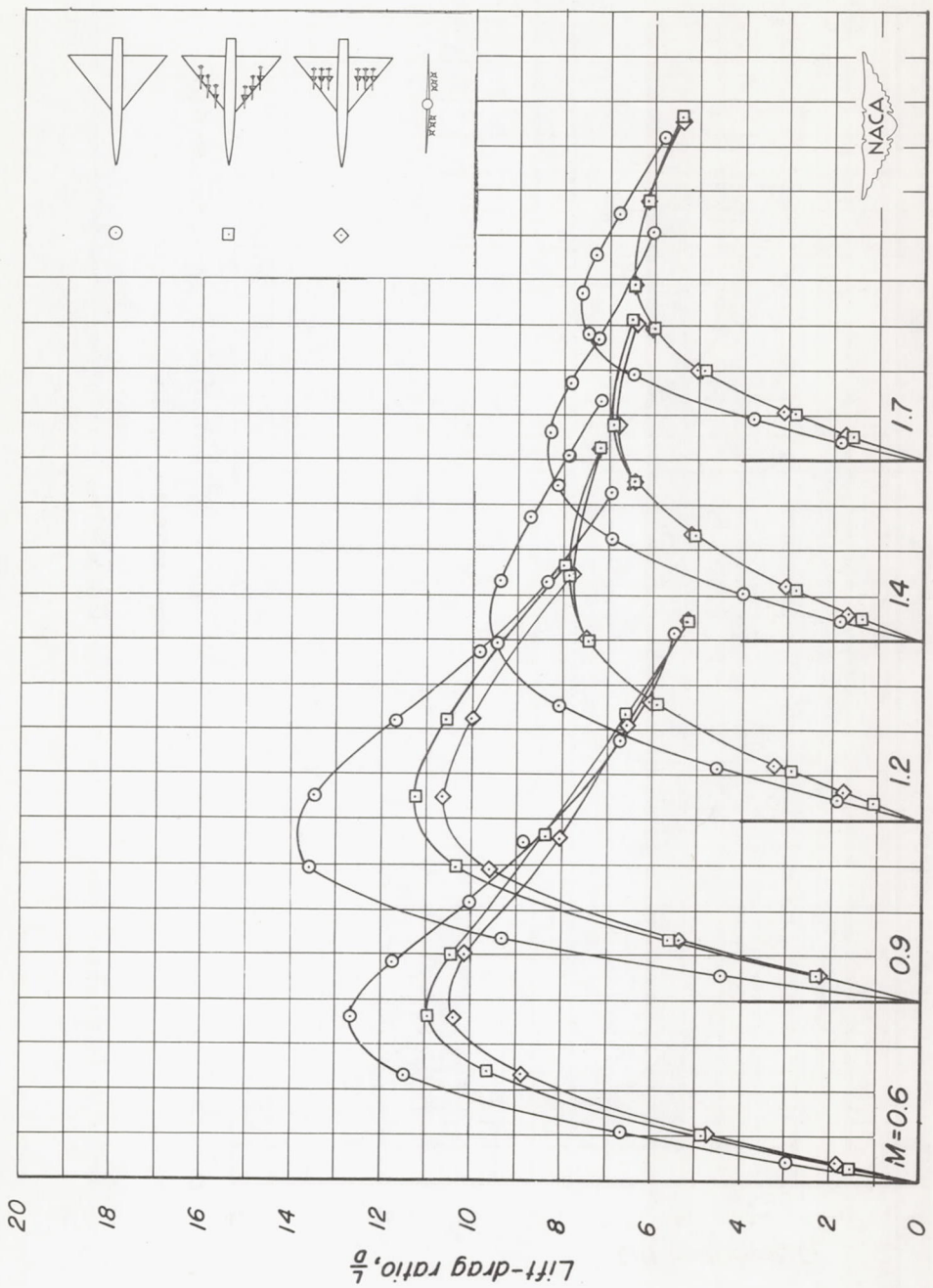
(b) C_L vs C_m

Figure 7.-Continued.



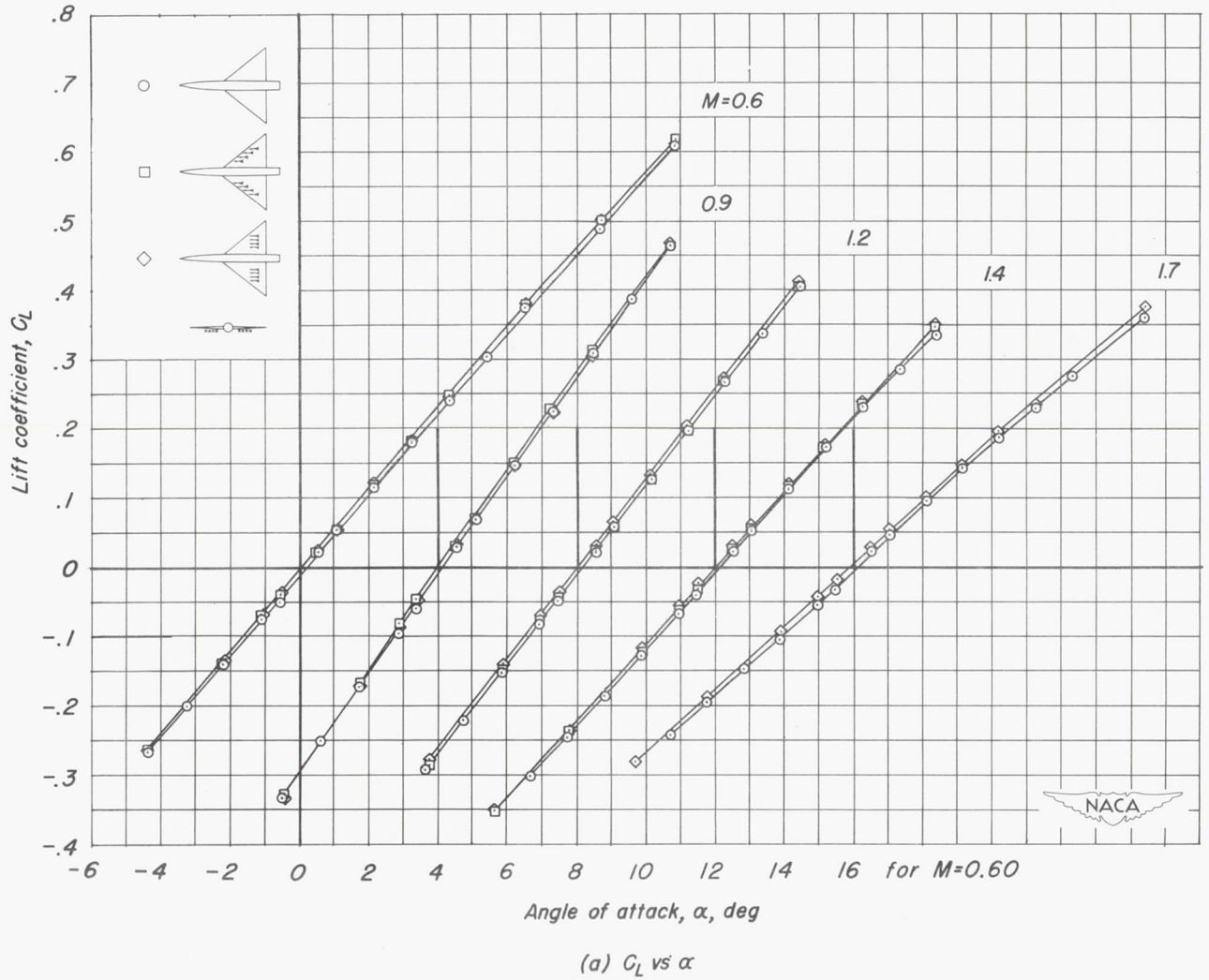
(c) C_L vs C_D

Figure 7 - Continued.



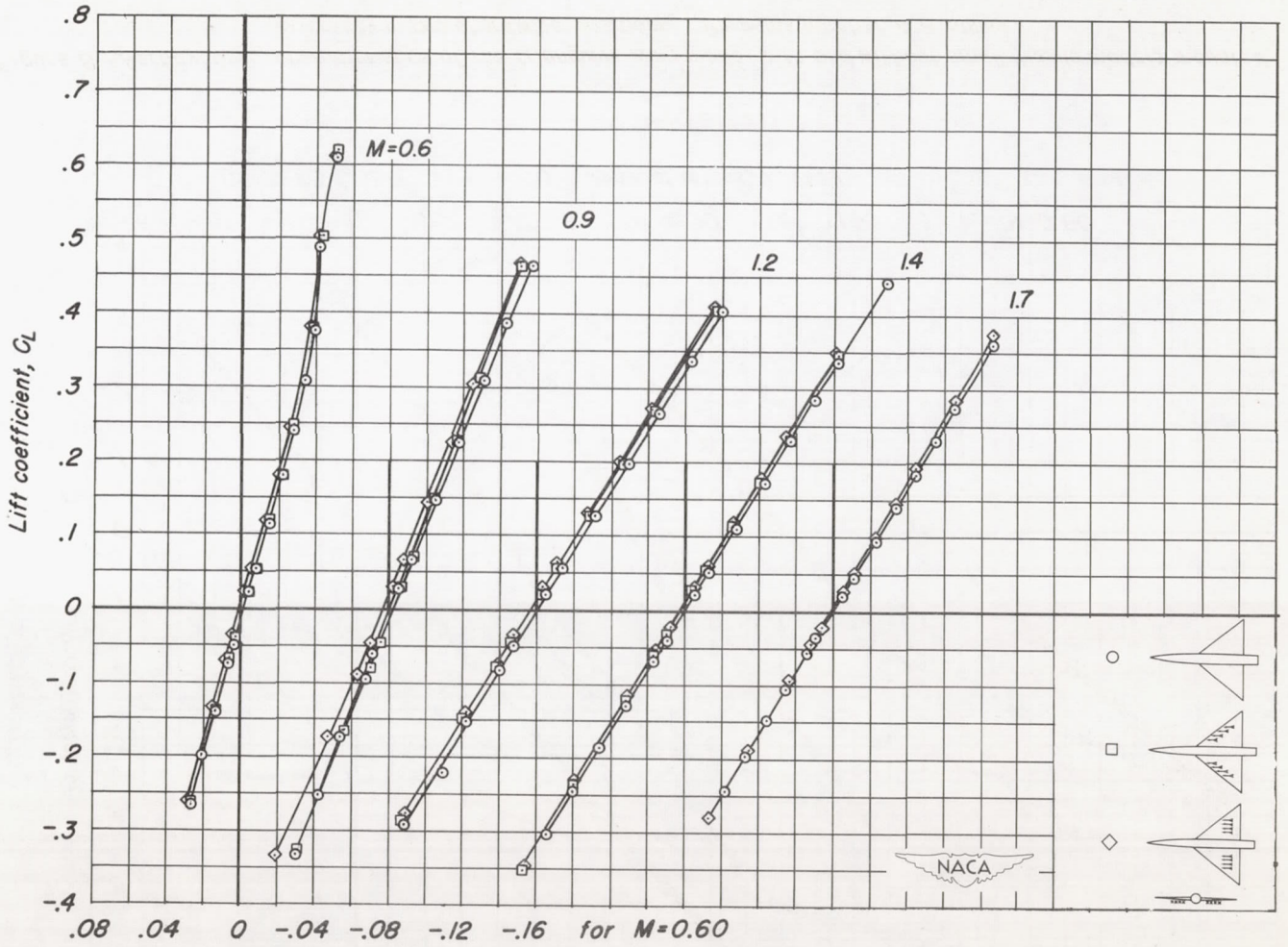
(d) C_L vs $\frac{L}{D}$

Figure 7.-Concluded.



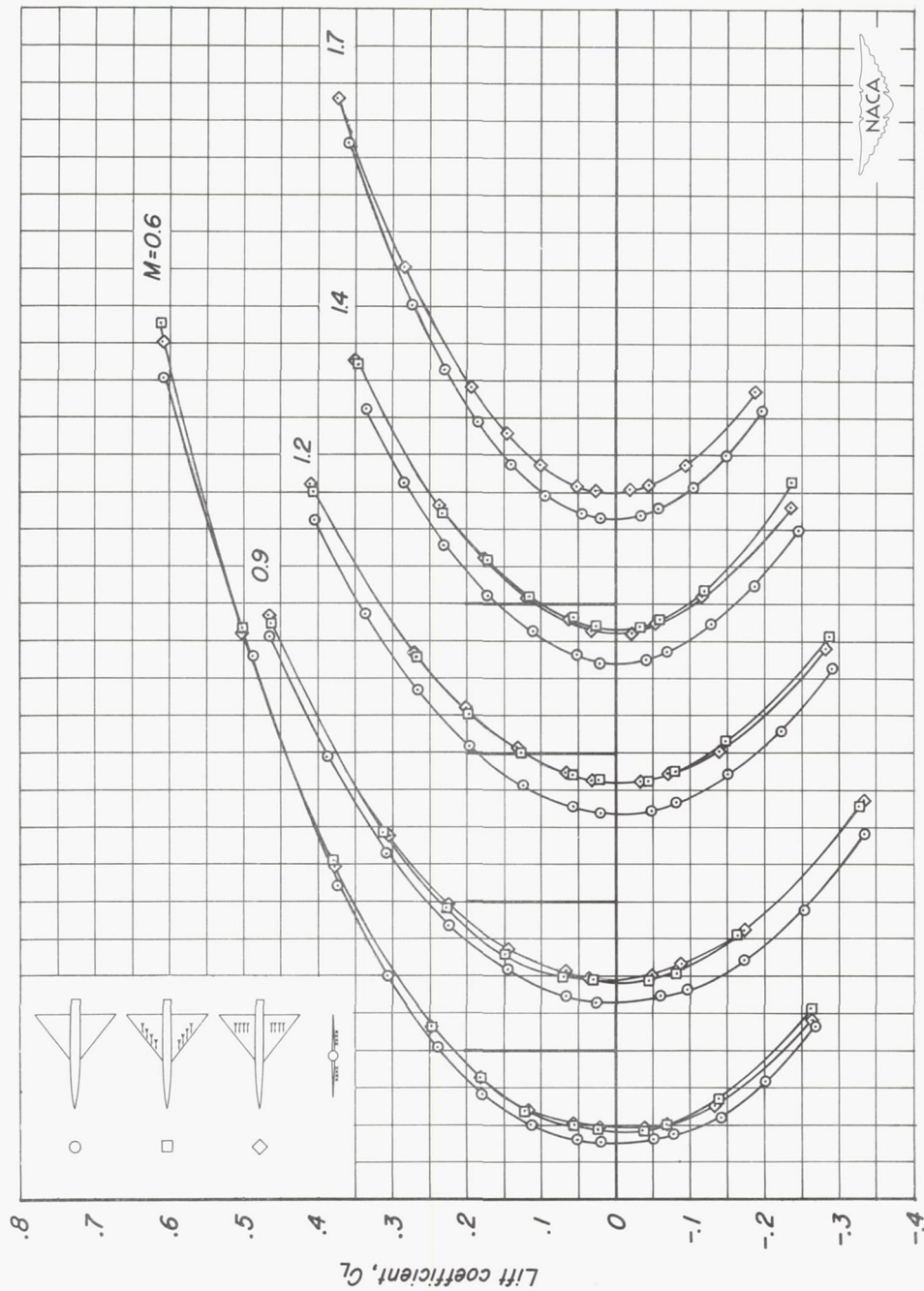
(a) C_L vs α

Figure 8.—Aerodynamic characteristics of the triangular wing model with and without small missile models mounted externally in two chordwise positions. Reynolds number, 4.8 million.



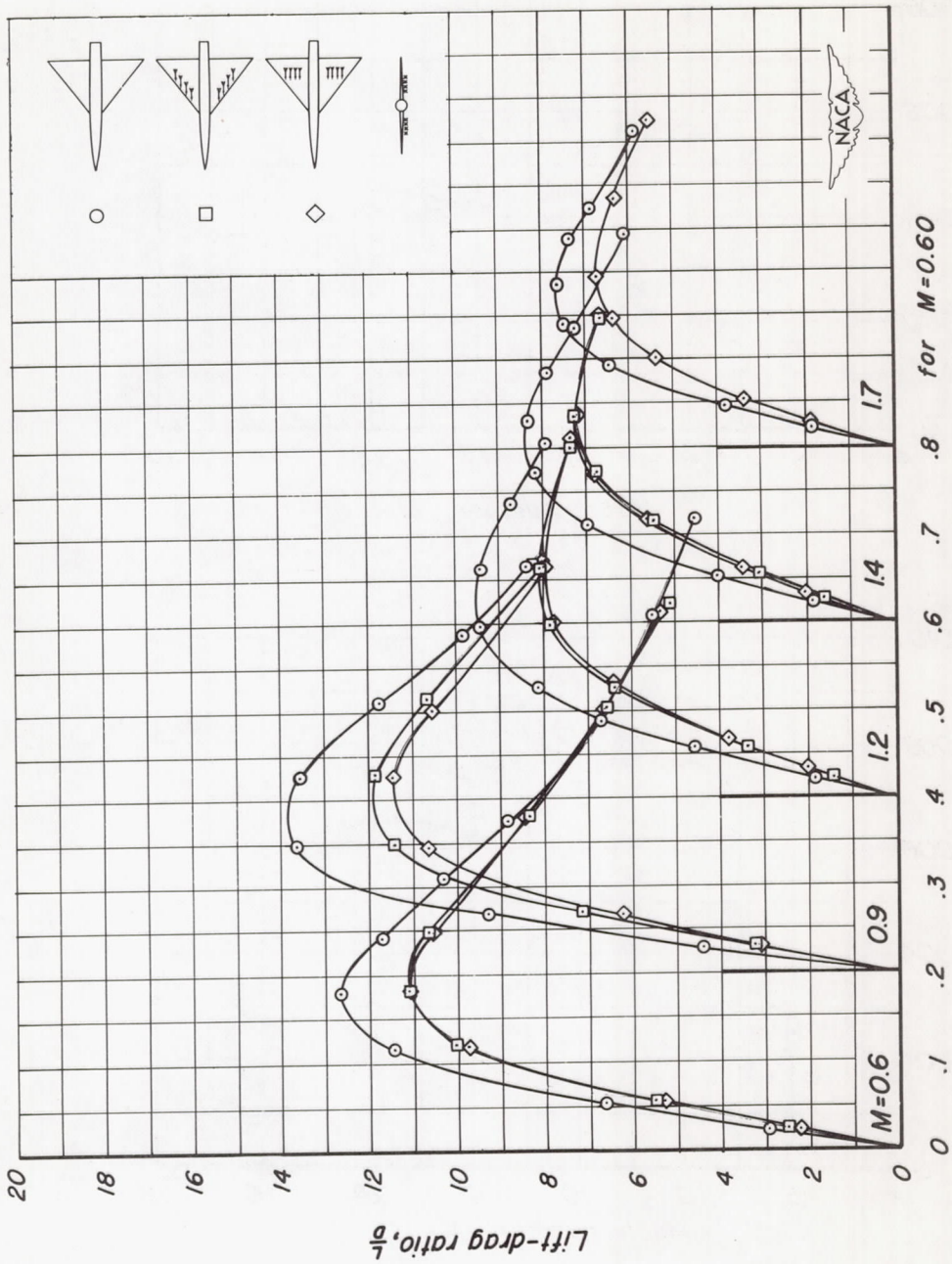
(b) C_L vs C_m

Figure 8.-Continued.



(c) C_L vs C_D

Figure 8.-Continued.



(d) C_L vs $\frac{L}{D}$

Figure 8.-Concluded.

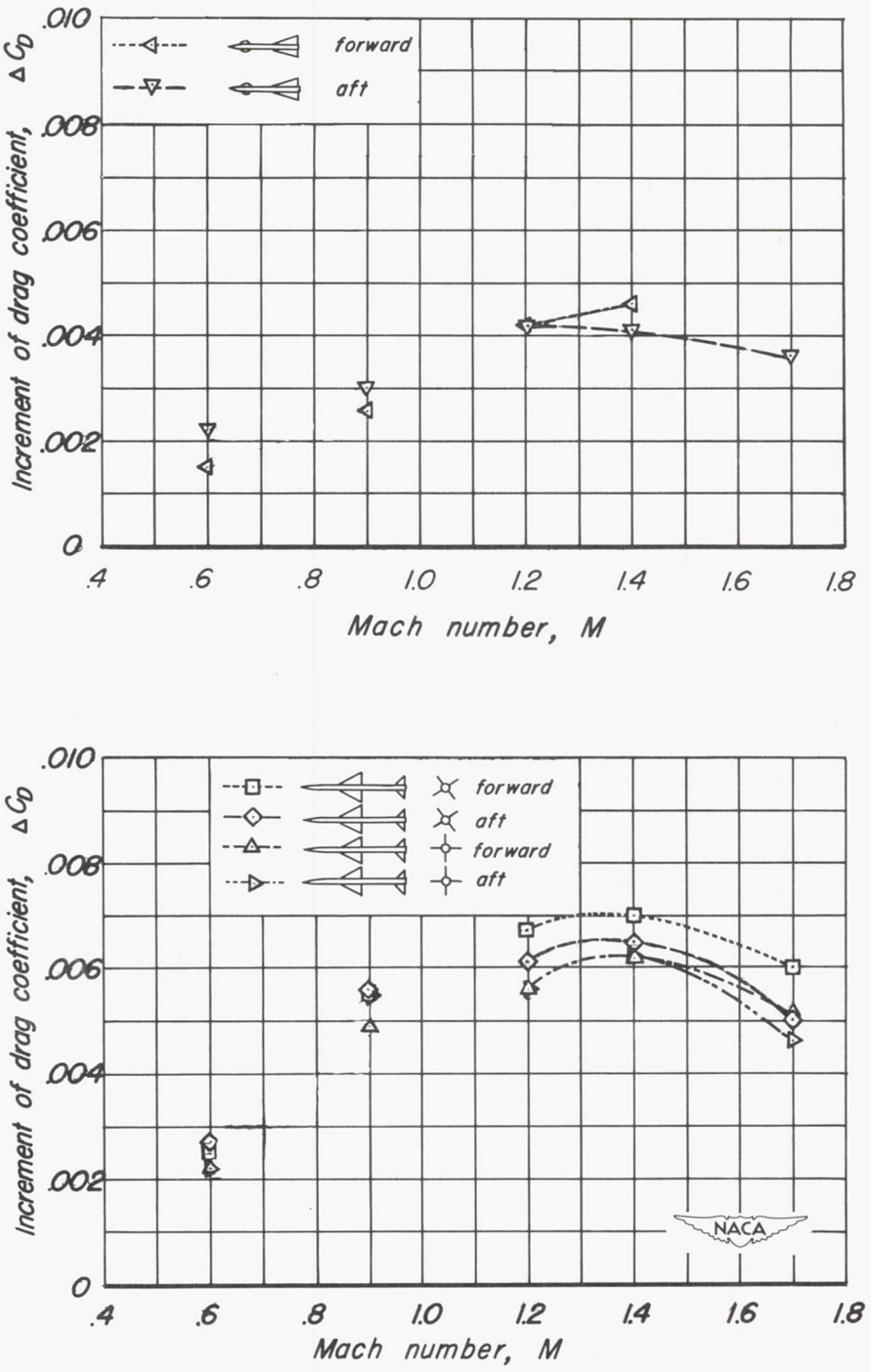


Figure 9. – Incremental drag coefficients for the missile models stored externally as a function of Mach number at zero lift. Reynolds number, 4.8 million.

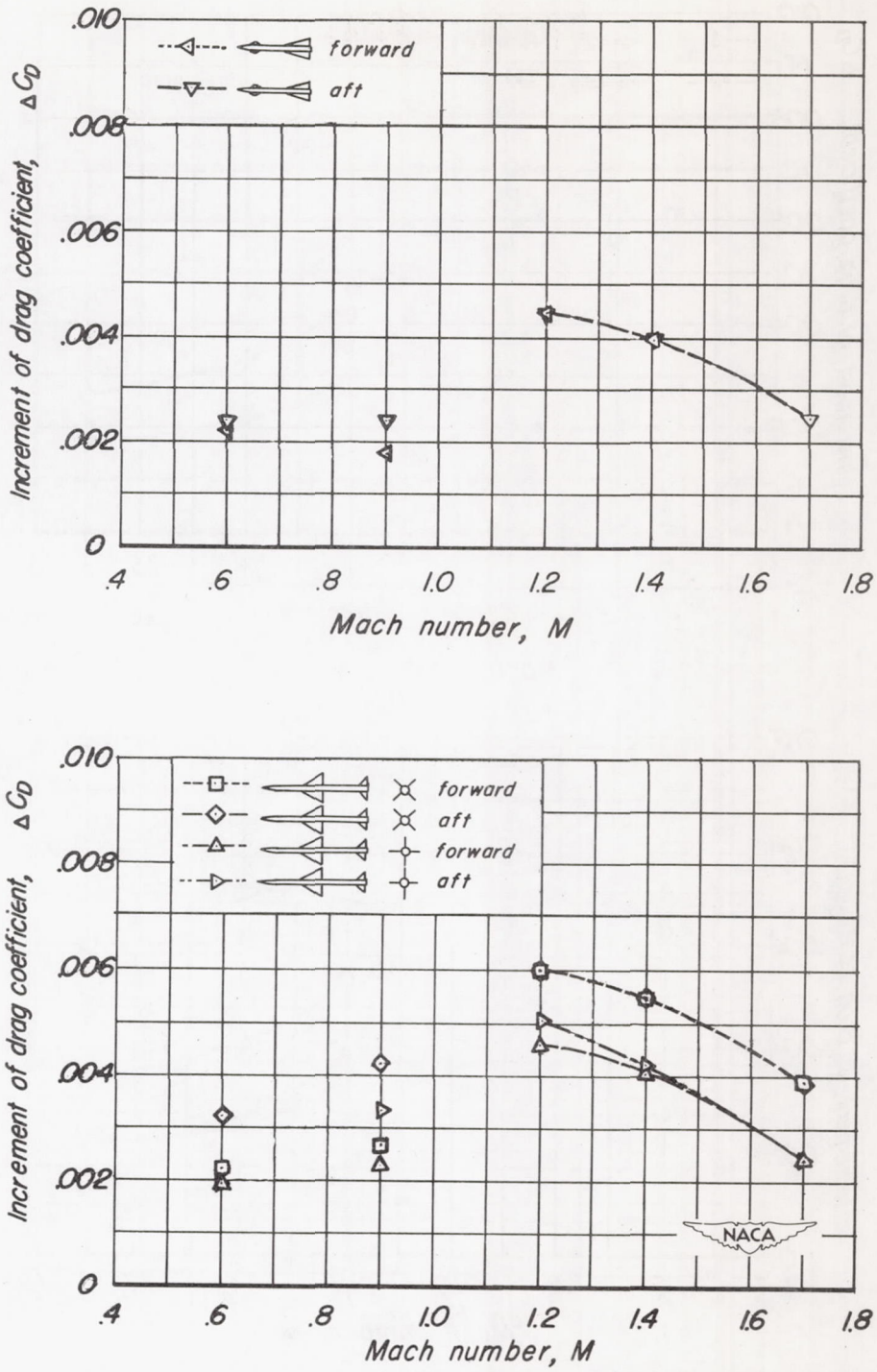


Figure 10. – Incremental drag coefficients for the missile models stored externally as a function of Mach number at a lift coefficient of 0.3. Reynolds number, 4.8 million.

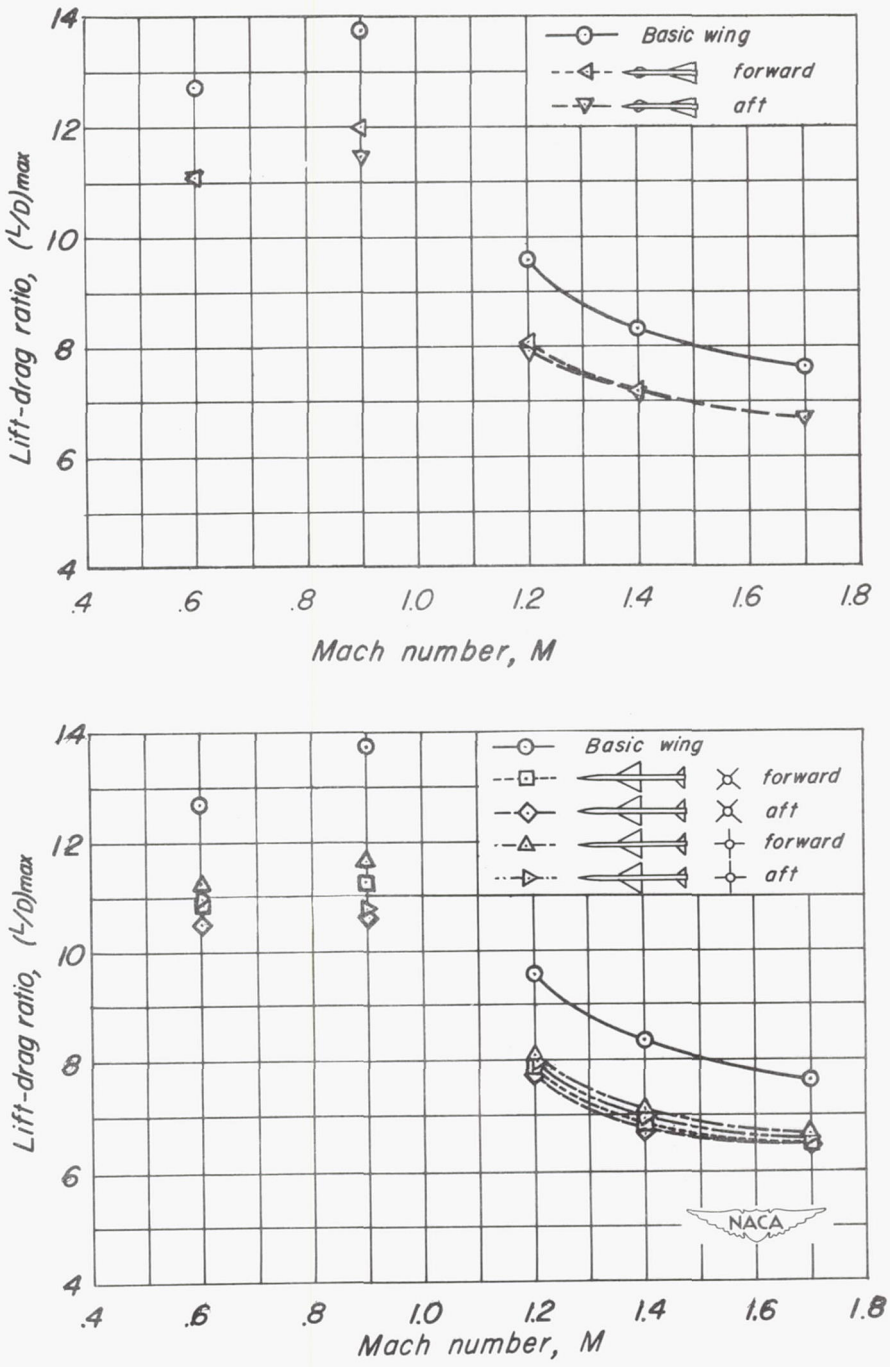


Figure 11. — Maximum lift–drag ratio for triangular wing with and without missile models stored externally as a function of Mach number. Reynolds number, 4.8 million.